Atomic Resolution Imaging on CeO$_2$(111) with Hydroxylated Probes

Sebastian Gritschneder[†] and Michael Reichling*

Fachbereich Physik, Universität Osnabrück, Barbarastraße 7, 49076 Osnabrück, Germany

Received: August 31, 2007; In Final Form: November 7, 2007

The formation of atomic contrast on the stoichiometric CeO$_2$(111) surface imaged by dynamic scanning force microscopy (SFM) operated in the noncontact mode (NC-AFM) is investigated. We reproducibly obtain two stable contrast patterns, namely a pattern of hexagonally ordered disk-like features and a honeycomb type structure. In series of measurements where we systematically vary the tip−surface distance, we find at a large distance exclusively disk-like contrast while the honeycomb pattern occasionally appears at a small tip−surface distance. We explain the contrast features within a model assuming that both types of contrast are created by the attractive interaction of first and third layer surface oxygen ions with the terminating cluster of the tip. We propose a tip model involving single or vicinal hydroxyl groups at the apex of a silicon oxide tip. Within this model, the disk like contrast is produced by the most protruding hydroxyl group while the reversible change in contrast found for a small tip−surface distance is caused by its relaxation and possibly further hydroxyl groups contributing to the tip sample interaction.

Introduction

Cerium dioxide (CeO$_2$, ceria) recently gained much attention for applications based on its remarkable catalytic properties.[1,2] Because of its high oxygen storage capacity, ceria is an important component of the three way catalyst used in automotive technology.[3] To gain insight into fundamental properties of this material, the CeO$_2$(111) surface has been investigated as a model surface by a wide range of experimental techniques addressing surface reactions[4−6] and phase transitions[7] as well as adsorption and desorption phenomena.[8−10] Among the experimental techniques applied, dynamic SFM is the only one capable of revealing surface structures in real space with atomic precision.[11,12] However, the interpretation of dynamic SFM data is not at all straightforward, as measured forces depend not only on atomic scale surface geometry but also on chemical and electrostatic interactions between the scanning tip and the surface that are hardly accessible. Therefore, a valid interpretation of atomic SFM contrast data cannot be deduced from a single image but has to be based on various pieces of evidence. Ideally, one piece of evidence is a quantum chemical simulation including SFM modeling as it has been demonstrated for the quantitative interpretation of contrast formation on the CaF$_2$-(111) surface.[13,14] In that work, the main finding was that contrast formation on fluorite is dominated by the polarity of the tip terminating ion assuming a polar tip that is best suited for imaging a strongly ionic material.

In this paper we present atomically resolved images of the CeO$_2$(111) surface aiming for an interpretation of contrast formation similar to the one obtained for CaF$_2$(111). For ceria, however, quantum chemical modeling and related SFM simulation is extremely difficult due to the challenge in modeling the 4f electron of cerium in existing codes, and a valid theoretical description of SFM imaging on CeO$_2$(111) is not yet available.

Therefore, we aim in this paper for an interpretation of the atomic contrast formation solely based on experimental evidence that has to be tested against theoretical results that hopefully will be available in the future.

Our initial approach was to take advantage of the intimate structural relationship between calcium difluoride (fluorite) and cerium dioxide, illustrated by the structural parameters compiled in Table 1 and to interpret the observed contrast pattern on CeO$_2$-(111) in analogy to the CaF$_2$(111) results. While the obtained contrast patterns are quite similar for both materials, we realize and outline below that the CaF$_2$ model does not yield a consistent interpretation of the contrast formation on CeO$_2$. Instead we propose that imaging on ceria can generally be explained by one type of tip termination and a change in contrast is not a result of a change in tip polarity but due to the interaction of the surface with a more complicated tip terminating structure. The tip model used to explain our results is based on an oxidized silicon tip with an apex covered by one or more hydroxyl species. This model can explain all images that we have recorded so far and is especially supported by a series of measurements involving a systematic variation of the tip−surface distance.

Results and Discussion

Experimental Findings. Experiments were performed with the same samples, setup, and experimental conditions used in our earlier studies.[15] Sample preparation included several cycles of Ar$^+$-ion sputtering and subsequent annealing of the surface at 900 °C according to the recipe published earlier.[16] After a successful preparation the surface, topography exhibits stacks of atomically flat hexagonal terraces and pits. For the present experiments, we have chosen annealing time and temperature to obtain large stoichiometric terraces that are virtually free of defects. The surface was scanned in the constant-height mode[11] with variations in the detuning of the cantilever oscillation reflecting the tip sample interaction. Note, that a more negative value of the detuning signal Δf corresponds to higher attractive interaction between tip and sample and is therefore displayed with brighter contrast in the SFM image. We used commercial
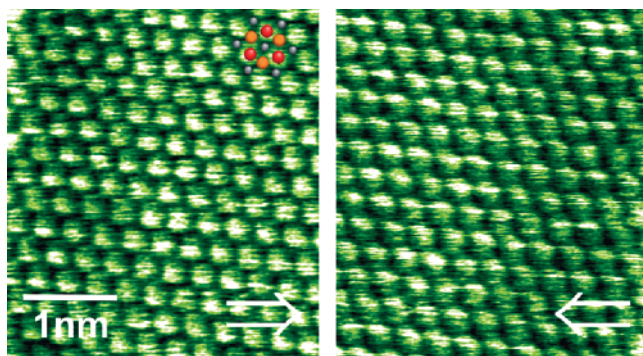
Figure 1. Detuning signal taken in forward (⟹) and backward (⟸) direction showing disk-like contrast, that is considered to be the standard contrast pattern. Images taken in forward and backward direction are identical, stable, very even and exhibit highly symmetric features pointing to imaging with a simple, highly symmetric tip. The model superimposed in the upper right corner of the left frame shows cerium ions, first layer oxygens and third layer oxygens by small gray, large red and large orange spheres, respectively.)

TABLE 1: Structural Parameters of CaF$_2$ and CeO$_2$ Single Crystals^a

material	lattice type/constant			ionic radius (nm)	
	type	a (nm)	nn (nm)	cation	anion
CaF$_2$	FCC	0.546	0.384	0.099 (Ca^{2+})	0.133(F$^-$)
CeO$_2$	FCC	0.541	0.382	0.092(Ce^{4+})	0.132(O^{2-})

^{a} a = lattice constant; nn = next neighbor distance.

silicon cantilevers with resonance frequencies of 60−75 kHz (PPP-QFMR, NanoWorld Services GmbH, Erlangen, Germany), that were oscillated with amplitudes of 25−40 nm. We did not treat the cantilever tips in any other way than to heat them in vacuum prior to experiments up to 120 °C for 50 h to remove contaminations. It can be anticipated that after such handling and treatment the apex of the silicon cantilever tip is covered by the native silicon oxide layer. We routinely achieve atomically resolved images with such tips and up to now we have recorded many hundreds of high quality atomically resolved images of the CeO$_2$(111) surface obtained under different experimental conditions. Therefore, we have an excellent statistical background for the analysis and interpretation of the observed contrast patterns. The conclusions drawn here are based on this large stock of consistent experimental results and not just on the representative images presented here.

As the standard atomic contrast on CeO$_2$(111), we obtain a disk-like pattern that directly represents the hexagonal surface structure with a lattice constant of 0.38 nm. Representative images exhibiting perfect regularity for forward and backward scanning are depicted in Figure 1. The perfect circular appearance of the disks representing surface ions and the regularity in contrast formation are a strong indication for a tip apex that is highly symmetric. Furthermore, there is no indication for any tip instability and we conclude that the apex of this tip is stable due to its very regular and symmetric atomic structure.[17]

The high regularity and stability of this tip is corroborated by results from a series of seven images taken with systematically increased average detuning of the cantilever oscillation, corresponding to a gradual reduction of the tip−surface distance. Three representative images from this series recorded at an average detuning of −9, −15, and −22 Hz, respectively, are shown in Figure 2. We find that the atomic corrugation increases linearly with detuning while the noise level decreases accordingly, but the disk-like contrast pattern is clearly present at all tip−surface separations. Note, that this series was recorded under
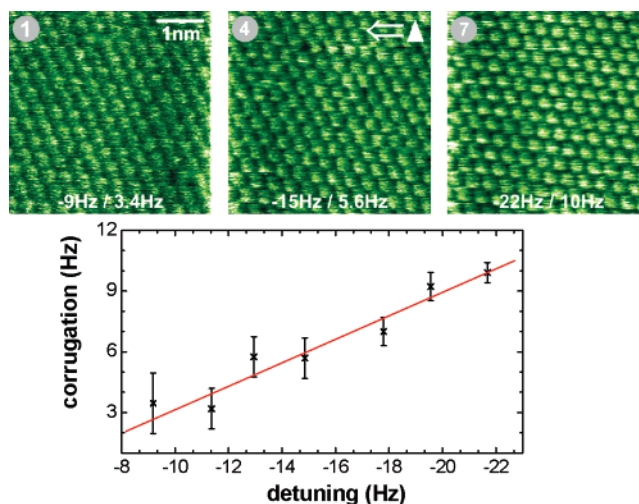

Figure 2. Representative images (frames 1, 4, and 7) from a series comprising seven measurements recorded with stepwise reduced tip−surface distance. These images were recorded with the same tip that has been used for recording the image of Figure 1. The arrows indicate the fast (⟸) and the slow (▲) scanning directions, respectively. Values for average detuning and atomic scale corrugation of the detuning signal are given for the selected frames and are plotted against each other in the graph. The straight line is the best linear fit to the data. We find that for a perfect tip the corrugation linearly increases with average detuning, while the disk-like contrast pattern is preserved throughout the approach series, even at very close tip−surface distances, where the corrugation is about half of the average detuning.
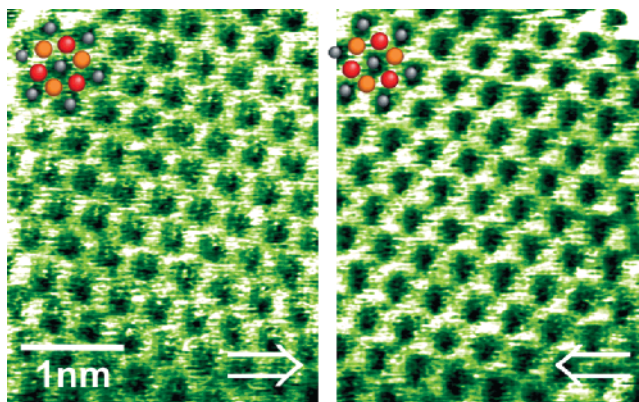

Figure 3. Detuning signal recorded in forward (⟹) and backward (⟸) direction showing honeycomb contrast. This pattern is obtained for a small fraction of images recorded at small tip surface distance. Slight differences in contrast formation between forward and backward direction point to a small asymmetry of the tip apex.

the most desirable imaging conditions with a perfect tip as it is available only in very few measurements. However, the main finding reported here, namely the prevalence of the disk like structure is clearly also found in many other measurements performed with slightly less regular tips.

In Figure 3 we present the only qualitatively different contrast pattern that we find for a much smaller fraction of images taken. This is a honeycomb pattern revealing dark spots surrounded by bright hexagonal structures. Imaging results from forward and backward scanning exhibit a very similar contrast, however, slight differences in the images point to a small asymmetry and instability of the tip apex. Unlike the disk-like contrast, the honeycomb pattern is found only at small tip−surface distance while any tip regardless of its structural details produces the disk-like contrast at large tip−surface distance. This type of contrast that has been observed for a number of measurements with a more asymmetric tip is examined in some detail for a
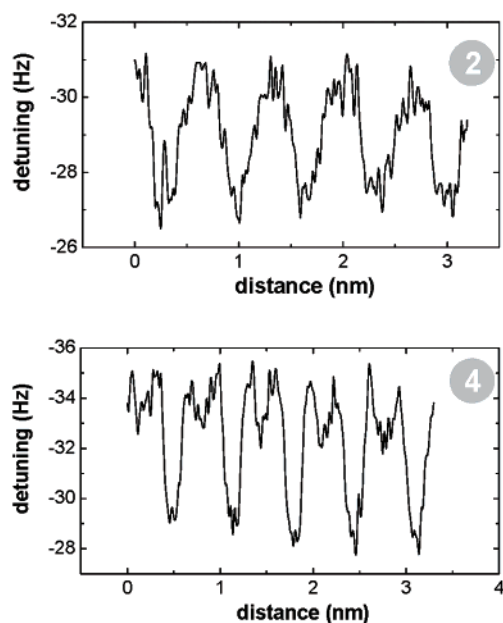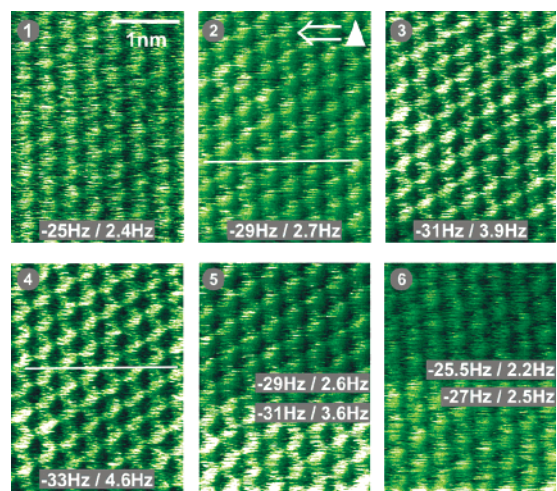
Atomic Resolution Imaging on CeO₂(111)

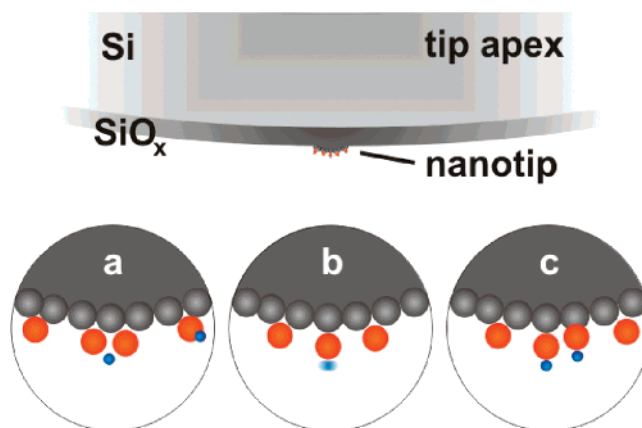*J. Phys. Chem. C, Vol. 112, No. 6, 2008* **2047**

Figure 5. Models of hydroxylated silicon oxide tips that could explain the observed atomic contrast. A firmly bound hydrogen as depicted in (a) is expected to produce the symmetric disk-like contrast as observed in the series of Figure 2. Tip structures shown in frames b and c are more flexible and complex facilitating the reversible change from the disk-like to the honeycomb pattern. In these cases, contrast formation is believed to be strongly influenced by dynamic relaxation of a loosely bound atom or double-tip effects.

Figure 4. Distance-dependent series of images recorded with a tip similar to the one used for obtaining the image of Figure 3. Average detuning and corrugation are given for each frame. In frames 5 and 6, the average detuning has been changed during taking the image. Disk-like contrast obtained at the beginning of the series, gradually turns into the honeycomb pattern, as the tip–surface distance is reduced. This change is reversible and the disk-like pattern as well as the corrugation is restored when the tip is retracted. Two line profiles taken in frames 2 and 4 along the [$\bar{2}$11] direction show the characteristic single peak structure for disk-like and the double peak structure for the honeycomb pattern.

series of measurements displayed in Figure 4. We show six representative frames taken from a series of measurements involving a systematic variation of the tip–surface distance. Frame 1 of the series has been recorded at a detuning of −25 Hz corresponding to a relatively large tip surface distance. For this frame we observe a disk-like contrast that is similar to the one of the standard image from Figure 1; however, a slight distortion of the disk-like pattern points to a small asymmetry or instability of the tip. Upon reducing the tip–surface distance, the contrast pattern changes gradually until it is turned into the honeycomb pattern at −33 Hz average detuning. Most importantly, the contrast pattern changes back to its disk-like appearance as we stepwise retract the tip from the surface in the second half of the experiment. Line profiles taken from corresponding frames of the series along the [$\bar{2}$11]-direction

exhibit the characteristic single peak for the disk-like and a double peak for the honeycomb pattern, respectively. The transition in contrast is best observed in frames 5 and 6 where we increased the tip–surface distance in an additional step in the middle of each frame. Note, that in the upper half of frame 6 we apply the same imaging conditions as in frame 1 and within the error of the measurement we reproduce the contrast pattern as well as the corrugation. We furthermore find that the transition between the two contrast patterns is not induced by a tip change that would appear as a horizontal line of instability in the detuning and dissipation (not shown) images, respectively. The absence of a tip change resulting in contrast inversion is also evident from earlier published measurements where we find that water molecules adsorbed on CeO₂(111) do not change their apparent contrast when the contrast found on the substrate changes from disk-like to honeycomb.[11]

Tip Model. The two presented distance dependent series of measurements comprise the essential experimental observations regarding contrast patterns on CeO₂(111) surfaces: the dominant contrast is a hexagonal pattern composed of disk-like bright spots, which can, depending on tip conditions, change into a honeycomb pattern at closer tip surface distance. Similar types of contrast patterns have already been observed on the structurally closely related CaF₂(111) surface[17] where a negative polarity results in disk-like contrast, while a positively terminated tip yields a triangular contrast turning into a honeycomb pattern at closer distance, respectively what is in direct contrast to the case of CeO₂(111) where we do not observe such tip changes that could explain the contrast behavior in line with the fluorite contrast model. Apart from the fact that the fluorite contrast model does not correctly describe the dynamic contrast formation in distance-dependent series of measurements, there is another observation that can hardly be explained by this model. In previous work we found that stable point defects and adsorbed water molecules are always imaged identically.[12] Point defects appear as dark spots at oxygen lattice sites while water molecules appear as bright protrusions at 3-fold oxygen hollow sites, regardless of the underlying lattice being imaged with disk-like or honeycomb contrast.[11] If the tip polarity would change, we would expect a contrast change that does not only affect the substrate but also the defects like it has recently been observed on the titania surface.[18] But neither tip changes during
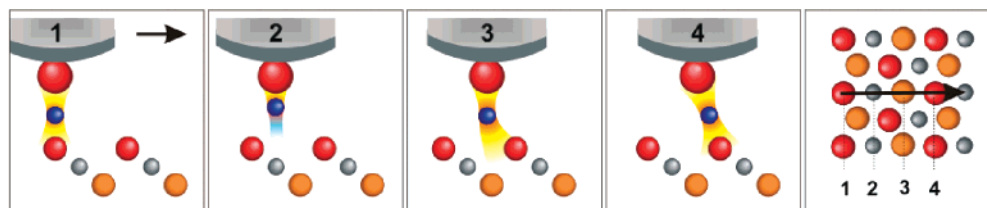
Figure 6. Series of four cartoons illustrating the formation of honeycomb contrast involving relaxation of a single hydroxyl at the tip apex while scanning along the [$\bar{2}$11] surface direction. The hydrogen end bends toward the next closest surface or subsurface oxygen ion (cartoon 1, 3, and 4), sensing an attractive force at all lateral positions, except directly above the cerium lattice site where the repulsive regime is dominating (cartoon 2). In the surface model on the right-hand side we assigned the cartoons to the corresponding situations during a line scan along the [$\bar{2}$11] direction.

the experiments nor other intended or unintended tip treatment results in a contrast change for these characteristic surface features. From these findings we conclude that the electrostatic properties are not subject to strong variation when scanning over ceria. Even after drastic tip changes, that are unavoidable during experiments, the imaging behavior of the tip remains similar, what implies that there is a preferential termination for the combination of the ceria surface with an oxidized silicon tip.

As plausible nanoscopic models for the tip apex, we propose clusters consisting of one or more hydroxyl groups terminating the oxidized tip with the hydrogen as the species creating atomic contrast pointing toward the surface. Such tip structures have already been investigated by theoretical simulation[19] and are schematically shown in Figure 5. It is known that a silicon tip exposed to ambient conditions is covered by a native oxide layer[20,21] that is very reactive to water adsorption and dissociation. Hence, any cantilever that is introduced into the UHV can be expected to be covered by water and a variety of water dissociation products like isolated, vicinal, and geminal silanols ($\equiv$SiOH). As silanols are only efficiently removed from silicon oxide surfaces at temperatures above 200 °C[21] and our cantilevers are not heated to temperatures higher than 120 °C, it can be anticipated that there is a notable amount of silanol groups present on the tip at the start of our experiments. On CeO$_2$(111) we routinely achieve atomic resolution without further manipulation of the tip apex so that it is justified to assume that a single silanol group sticking out of the tip yields the atomic contrast. Within this model, the positive potential of the hydrogen pointing toward the surface experiences an attractive force above ions of the anionic sub-lattice that are imaged as bright spots. Imaging results shown in Figures 1 and 2 represent the ideal case where the tip apex is formed by a nanotip with a symmetrically coordinated and firmly attached hydrogen as shown in Figure 5a. The intuitively expected quantitative increase of contrast with reduced tip surface distance is confirmed by the experimental observation. The reversible transition in contrast to the honeycomb pattern, as observed in results from Figures 3 and 4 can be explained by probing the surface with less stable and/or less well-defined hydroxylated tips as sketched in frames b and c of Figure 5.

In these cases, the tip-surface interaction presumably results in a relaxation of the nanocluster at the tip apex as it has been suggested by theoretical simulations.[22] A possible scenario of relaxation during a scan over Ce^{4+} ion and adjacent first and third layer O^{2-} ions is illustrated by the four cartoons shown in Figure 6. Assuming that the imaging hydrogen is not too strongly bound to the tip apex, it will at close tip−sample distances bend toward the nearest surface oxygen (see cartoon 1 and 4) and may also be affected by the attraction of third layer oxygen ions (cartoon 3). In that way, the tip senses at all positions except directly on top of the cerium ions an attractive force while there is a repulsive component above the cerium ion (cartoon 2). The overall result is the observed honeycomb

pattern with bright contrast above surface and subsurface oxygen ions and dark contrast above cerium ions. As the silanol density is expected to amount to 2.8 OH-groups per nm^2,[21] we suggest that in the general case additional silanols may be located in the closest vicinity to the main probe (see Figure 5c). While their contribution to the overall tip−sample force may be negligible at large distances, these secondary probes certainly play a significant role at closer tip−sample distances. Depending on the relative position of the additional silanols with respect to the main probe, the honeycomb pattern may become asymmetric and distorted as it is the case for the images from Figures 3 and 4.

Conclusion

Dynamic SFM imaging on CeO$_2$(111) regularly yields two kinds of contrast, a disk-like and a honeycomb pattern, are regularly observed. We find that contrast patterns are similar to earlier obtained images of the structurally closely related CaF$_2$(111) surface, however, clearly realize that the observed phenomena of contrast formation are distinctively different. These differences are caused by differences in the chemical composition of the tip apex present during imaging the two materials. In the case of fluorite, strong atomic contrast is not obtained until the tip has picked up material from the surface. As a result the chemically inert fluorite surface is imaged with an inert fluorite cluster, and the contrast mechanism is dominated by the polarity of the tip terminating ion. In the case of ceria, the tip apex consists of an oxide cluster. This is either silicon oxide or ceria if sample material is picked up. Hence, in this case a reactive oxide surface is imaged with a reactive oxide tip. Such an oxide tip will rapidly react with water from the residual gas of the UHV or during handling the tip outside the vacuum and dissociation will readily produce hydroxyl groups. These hydroxyl groups are the dominant species on the tip apex and completely determine atomic contrast formation on the oxide. This explains the predominance of one type of contrast on ceria and the absence of any images indicating another tip termination.

References and Notes

(1) Trovarelli, A.; de Leitenburg, C.; Boaro, M.; Dolcetti, G. *Catal. Today* **1999**, *50*, 353.

(2) Bernal, S.; Kaspar, J.; Trovarelli, A. *Catal. Today* **1999**, *50*, 173.

(3) Gandhi, H. S.; Graham, G. W.; McCabe, R. W. *J. Catal.* **2003**, *216*, 433.

(4) Henderson, M. A.; Perkins, C. L.; Engelhard, M. H.; Thevuthasan, S.; Peden, C. H. F. *Surf. Sci.* **2003**, *526*, 1.

(5) Al-Madfa, H. A.; Khader, M. M.; Morris, M. A. *Int. J. Chem. Kinet.* **2004**, *36*, 293.

(6) Pushkarev, V. V.; Kovalchuk, V. I.; d'Itri, J. L. *J. Phys. Chem. B* **2004**, *108*, 5341.

(7) Xiao, W.; Guo, Q.; Wang, E. G. *Chem. Phys. Lett.* **2003**, *368*, 527.

(8) Namai, Y.; Fukui, K.-i.; Iwasawa, Y. *Nanotechnology* **2004**, *15*, S49.

(9) Luo, M. F.; Zhong, Y. J.; Zhu, B.; Yuan, X. X.; Zheng, X. M. *Appl. Surf. Sci.* **1997**, *115*, 185.

(10) Bulanin, K. M.; Lavalley, J. C.; Lamotte, J.; Mariey, L.; Tsyganenko, N. M.; Tsyganenko, A. A. *J. Phys. Chem. B* **1998**, *102*, 6809.

(11) Gritschneder, S.; Reichling, M. *Nanotechnology* **2007**, *18*, 044024.

(12) Gritschneder, S.; Iwasawa, Y.; Reichling, M. *Nanotechnology* **2007**, *18*, 044025.

(13) Foster, A. S.; Barth, C.; Shluger, A. L.; Reichling, M. *Phys. Rev. Lett.* **2001**, *86*, 2373.

(14) Barth, C.; Foster, A. S.; Reichling, M.; Shluger, A. L. *J. Phys.-Condensed Matter* **2001**, *13*, 2061.

(15) Gritschneder, S.; Namai, Y.; Iwasawa, Y.; Reichling, M. *Nanotechnology* **2005**, *16*, S41.

(16) Fukui, K.-I.; Namai, Y.; Iwasawa, Y. *Appl. Surf. Sci.* **2002**, *188*, 252.

(17) Foster, A. S.; Barth, C.; Shluger, A. L.; Nieminen, R. M.; Reichling, M. *Phys. Rev. B* **2002**, *66*, 235417.

(18) Lauritsen, J. V.; et al., *Nanotechnology* **2006**, *17*, 3436.

(19) Foster, A. S.; Shluger, A. L.; Nieminen, R. M. *Nanotechnology* **2004**, *15*, S60.

(20) Henderson, M. A. *Surf. Sci. Rep.* **2002**, *46*, 1.

(21) Zhuravlev, L. T. *Colloids Surf. A* **2000**, *173*, 1.

(22) Pakarinen, O. H.; Barth, C.; Foster, A. S.; Nieminen, R. M.; Henry, C. R. *Phys. Rev. B* **2006**, *7323*, 5428.